Photocatalysis

DOI: 10.1002/anie.201304481

Direct Four-Electron Reduction of O_2 to H_2O on TiO_2 Surfaces by Pendant Proton Relay**

Hua Sheng, Hongwei Ji, Wanhong Ma, Chuncheng Chen, and Jincai Zhao*

TiO_2-based photocatalytic aerobic oxidations are among the most promising methods in energy conversion, environmental remediation, and organic transformation by using solar energy.[1–4] In the photocatalytic reactions, oxygen acts as the ultimate oxidant by scavenging conduction-band electrons, and the oxygen reduction reaction (ORR) carried out by conduction band electrons is the key step, even the rate-determining step, of the overall reactions.[1] During ORR, various reactive oxygen species (i.e. $^{\bullet}OH$, H_2O_2, $O_2^{\bullet-}$) are generated which are able to strongly influence the reaction mechanisms and product distribution.[1,5] For example, in our previous study, the $^{\bullet}OH$ derived from the H_2O_2 intermediates of ORR can contribute much to the hydroxylation of aromatics.[6]

It is generally accepted that, on TiO_2 surface, ORR proceeds by a series of sequential single-electron reduction reactions and concomitantly with the formation of various reactive oxygen species [Eqs. (1)–(5); cb = conduction band,

$$TiO_2 + h\nu \rightarrow e_{cb}^- + h_{vb}^+ \quad (1)$$

$$O_2 + e_{cb}^- \rightarrow O_2^{\bullet-} \quad (2)$$

$$H^+ + O_2^{\bullet-} \rightarrow HO_2^{\bullet} \ (pH < 4.8) \quad (3)$$

$$2\,HO_2^{\bullet} \rightarrow H_2O_2 + O_2 \quad (4)$$

$$HO_2^{\bullet} + e_{cb}^- + H^+ \rightarrow H_2O_2 \quad (5)$$

vb = valence band]. Among them, intermediate H_2O_2 is almost always accumulated in a considerable amount owing to its relative stability.[7] On the other hand, these active oxygen species could be avoided, if the ORR proceeded by a direct four-electron pathway. However, control of the oxygen reduction pathway on the photocatalyst surface remains a great challenge, and only limited progress has been made to date. It was reported that, for example, loading Au nanoparticles[8] or copper ions[9] onto the TiO_2 surface could drastically enhance photocatalytic generation of H_2O_2 from O_2.

[*] Dr. H. Sheng, Prof. H. Ji, Prof. W. Ma, Prof. C. Chen, Prof. J. Zhao
Key Laboratory of Photochemistry, Beijing National Laboratory for Molecular Sciences, Institute of Chemistry
The Chinese Academy of Sciences
Beijing, 100190 (China)
E-mail: ccchen@iccas.ac.cn

[**] We appreciate the financial support by the 973 project (2010CB933503, 2013CB632405) and by the NSFC (No. 21137004, 21077110 and 21277147).

Supporting information for this article is available on the WWW under http://dx.doi.org/10.1002/anie.201304481.

ORR becomes more efficient when the electron transfer is coupled with the transfer of proton, the so-called proton-coupled electron transfer (PCET) process.[10,11] Despite extensive investigations in the homogeneous organic phase,[10,12,13] the importance of PCET for the ORR on metal oxide surface is seldom demonstrated. Actually, the essential role of proton in the reduction process on the metal oxides (TiO_2 and ZnO) was recognized by Mayer et al. only very recently.[14]

Inspired by the depressed formation of H_2O_2 in the presence of phosphate during photocatalytic oxidation of aromatics, herein, we demonstrate that the reduction pathway of O_2 on a TiO_2 surface is switched from a sequential single-electron process to a concerted $4\,e^-/4\,H^+$ reduction to H_2O by simply adding pendant proton relays (polyprotic acids). In contrast, monocarboxylic acids without pendant proton relays only enhance the ORR reduction rate but barely change the reaction pathway. Our work highlights the important role of acid/base relays in tuning ORR and consequently the overall photocatalytic pathway on metal oxide surface.

Our first interesting observation came from the marked influence of phosphate on the photocatalytic behavior of TiO_2 during the oxidation of benzoic acid (BA). It was observed that the rate for the photocatalytic degradation of benzoic acid (BA) was significantly enhanced after addition of phosphate at the same pH value. The apparent zero-order rate constant increased from 45 $\mu M\,min^{-1}$ on pristine TiO_2 to 110 $\mu M\,min^{-1}$ in the phosphate system (Figure 1a left axis). More intriguingly, a sharp contrast in the H_2O_2 accumulation was observed between pristine and phosphate-modified TiO_2. The H_2O_2 concentration in the pristine TiO_2 system (71.8 μM) was approximately 40 times higher than in the phosphate system (only 1.7 μM) after irradiation for 120 min, and still increasing with the photocatalytic conversion (Figure 1a right axis). The concentration of H_2O_2 is determined by its formation [Eqs. (1)–(5)] and decomposition [Eqs. (6)–(8)]

$$H_2O_2 + e_{cb}^- \rightarrow OH^- + {}^{\bullet}OH \quad (6)$$

$$H_2O_2 + 2\,e_{cb}^- + 2\,H^+ \rightarrow 2\,H_2O \quad (7)$$

$$H_2O_2 + 2\,H_{vb}^+ \rightarrow O_2 + 2\,H^+ \quad (8)$$

kinetics under photocatalytic conditions. A control experiment on the photocatalytic decomposition of H_2O_2 (0.1 mM) showed that the pseudo-zero-order decay rate constant of H_2O_2 in the presence of PO_4^{3-} was much less than that in the pristine TiO_2 system (1.34 vs 4.62 $\mu M\,min^{-1}$, Figure S1 in the Supporting Information), probably because of blocking of the interaction of H_2O_2 with the TiO_2 surface by the surface-

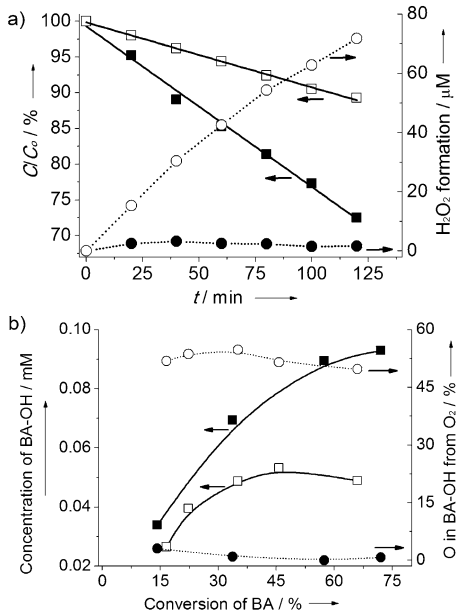

Figure 1. a) Influence of phosphates on the oxidation rates (left axis) and the accumulation of H_2O_2 (right axis) during photocatalytic degradation of benzoic acid under UV irradiation at pH 3.5; C = concentration of BA, C_o = initial concentration of BA. b) Influence of phosphates on the yield of the hydroxylated products BA-OH (left axis) and the oxygen atom source of hydroxy group in BA-OH (right axis) during BA degradation, using aerial $^{16}O_2$ as the oxidant and $H_2{}^{18}O$ (90%) as the solvent. For both panels, □/○: pristine TiO_2; ■/●: TiO_2 with 2 mM phosphates.

bound phosphates. Therefore, the lack of H_2O_2 accumulation, in spite of the enhanced conversion of BA, indicates that the generation of H_2O_2 on the surface with phosphates was remarkably suppressed.

Recent studies showed that the oxygen atoms in the OH groups of the hydroxylated products during the photooxidation of aromatics can be derived from both the oxidant O_2 and solvent H_2O [Eq. (9)],[15] and their relative percentage

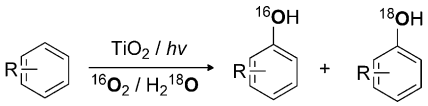

(9)

depends largely on the reaction mechanism.[6] To show the influence of phosphate on the mechanism, the relative importance of these two oxygen sources in the OH group of the hydroxylated products (BA-OH) was further probed by isotope-labeling analysis ($^{16}O_2$ and $H_2{}^{18}O$). As shown in Figure 1b, for pristine TiO_2, as much as 50% of the O-atoms of hydroxy groups in BA-OH were derived from O_2. In sharp contrast, almost no O-atoms from O_2 were detected in the products formed by the phosphate system. To rule out the effect of the changed adsorption of BA by phosphates, the photocatalytic oxidation of weakly adsorbed benzene was also examined. Similar to the oxidation of BA, a significantly decreased O-atom incorporation from O_2 into phenol was also observed upon addition of phosphate (from about 50% to 10%, Figure S2). We recently showed that photocatalytic O-incorporation from O_2 into hydroxylation products is through the intermediate H_2O_2.[5] Our present observation of the reduced O-incorporation from O_2 in the presence of PO_4^{3-} indicates the formation of active oxygen species H_2O_2, $^{\bullet}OH$, and $O_2^{\bullet-}$ by consecutive $1e^-$-reduction of O_2 [Eqs. (1)–(5)] is largely inhibited by adsorbed phosphates, which is in line with the H_2O_2 measurements.

The analysis of the yield of the hydroxylated products showed that the product distribution also changed significantly upon addition of phosphate. The yield of the hydroxylated intermediates (ratio of the detected BA-OH/phenol to the consumed BA/benzene) was much higher in the phosphate systems than in the pristine TiO_2 (Figure 1b, Figure S2). The decrease of O_2-derived active radicals, together with previously reported $^{\bullet}OH$ enhancement in the presence of phosphates,[16–18] should be responsible for the higher yield of hydroxylated intermediates.

The depressed H_2O_2 generation and O-atom-incorporation from O_2 during the photocatalytic reactions implies a significant change in the oxygen reduction processes on the TiO_2 surface in the presence of phosphates. To avoid the complicated redox processes under photocatalytic conditions and to shed light specifically on the reduction of oxygen, the ORR was further examined on the TiO_2 film electrode at bias potentials. Using TiO_2 film as working electrode, linear sweep voltammetry (LSV) of the ORR was first examined at pH 3.5. As shown in Figure 2a, in Ar-saturated solutions, little current was observed regardless of the presence of phosphates, while in O_2-saturated solutions, a reduction current with onset at about −0.45 V (vs. saturated calomel electrode (SCE)) was

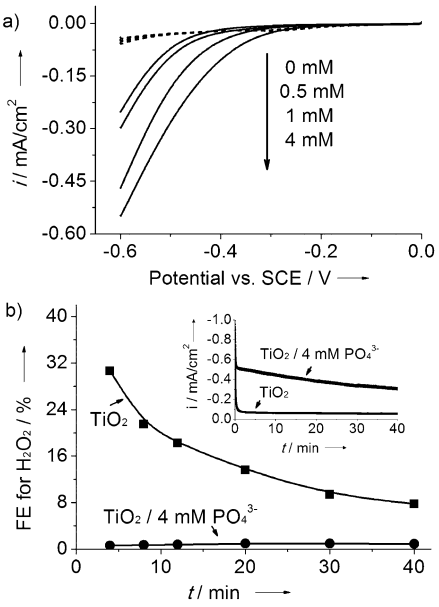

Figure 2. a) Linear sweep voltammetry (50 $mV s^{-1}$) of a TiO_2 film in Ar (dashed lines) or O_2-saturated (solid lines) 0.1 M $NaClO_4$ solutions in the absence of or the presence of the concentrations of phosphate shown. b) Faradaic efficiency (FE) for H_2O_2 during the steady-state electrolysis at −0.5 V (vs. SCE) for TiO_2 film in the absence of or the presence of 4 mM PO_4^{3-} in O_2-bubbled 0.1 M $NaClO_4$ electrolyte (pH 3.5). Inset: the corresponding ready-state reduction current density.

observed, indicating oxygen reduction occurring on the TiO_2 surface. With increased phosphates concentrations, the current density also increased, and the onset gradually shifted to a more positive potential. For instance, after addition of 4 mM phosphates, the cathodic current density at −0.5 V increased four times, and the onset potential positively shifted about 200 mV, indicating that the addition of phosphates is able to promote ORR on TiO_2 surface.

Figure 2b shows the steady-state reduction current density and the Faradaic efficiency ($FE = n_{H_2O_2}/2n_e$) for H_2O_2 over time on the TiO_2 electrode in the absence and presence of 4 mM phosphates at −0.5 V (vs. SCE) in a two-compartment electrochemical cell. Consistent with the LSV results, the steady-state reduction current density was much higher in the phosphate system than in the pristine one. The reduction current increased 10–15 times in the presence of phosphates at potential of −0.5 V (Figure 2b inset), which, once again, demonstrates the improved ORR activity of phosphate-anchored TiO_2. As shown in Equations (1)–(5), on the pristine surface, the single-electron transfer ORR would lead to the accumulation of considerable amount of intermediate H_2O_2,[7] which can be considered as the indicator to judge the ORR pathway. The detected FE of H_2O_2 on the pristine surface was about 31% after electrolysis for 4 min. The overall FE drops gradually with the time, probably owing to the further reduction of the formed H_2O_2. In sharp contrast, when the electrode was immersed in the phosphate-containing electrolyte, the FE of H_2O_2 was only 0.6%, and did not change much over time.

A control experiment on the electrolytic decomposition of H_2O_2 under Ar atmosphere showed that the presence of phosphates hindered the decomposition of H_2O_2 with an apparent first-order decay rate constant declining from 0.064 to 0.029 min^{-1} (Figure S3), which is in line with the photocatalytic decomposition of H_2O_2 (Figure S1). That there is little H_2O_2 accumulation in the presence of phosphate, in spite of the decreased decomposition of H_2O_2 and the increased reduction of O_2, confirms that O_2 in the phosphates systems is selectively reduced to H_2O, while the pathway of the sequential single-electron reduction to H_2O_2 is bypassed. Moreover, the preadsorbing experiment (see Supporting Information) confirms that the effect of PO_4^{3-} on the ORR of TiO_2 is a result of the surface-bound anions, rather than those in the bulk solution.

The four-electron pathway of ORR in the presence of phosphates was further confirmed by rotating disc electrode (RDE) experiments. As shown in Figure S4, for pristine TiO_2, the typical two-step pathway at around −0.45 V and −1.0 V was observed, indicating a successive single-electron reduction [Eqs. (2)–(7)]. Interestingly, with the increased addition of PO_4^{3-}, the first reduction plateau became less pronounced and gradually vanished. The LSV curves finally showed a single-step plateau in the presence of 4 mM PO_4^{3-}, indicating a direct four-electron ORR process. Using the Koutecky–Levich equation, the overall number of the transferred electrons (n) in the ORR at plateau currents was quantitatively estimated, the result is shown in Figure 3. The value n was calculated to be approximately 2 on pristine TiO_2, with the addition of PO_4^{3-}, the n values gradually increased. In the presence of 4 mM PO_4^{3-}, n reached 4, indicative of the four-electron path, which is consistent with the higher ORR current density and lower FE of H_2O_2 observed for phosphate-modified TiO_2.

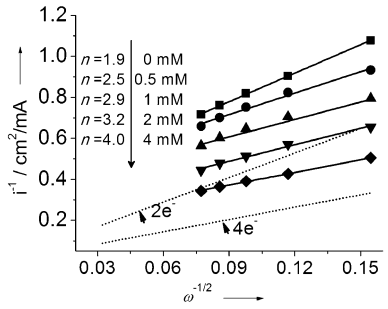

Figure 3. Koutecky–Levich plots of a TiO_2 film immersed in different concentrations of phosphates at plateau currents. The dashed lines show the standard slopes for $n = 2$ and $n = 4$.

The phosphates and organic acids are good proton relays to enhance many proton-coupled electron transfer (PCET) processes.[19,20] Recently, the reduction of phenoxyl and nitroxyl radicals on the surface of reduced TiO_2 and ZnO was also demonstrated to proceed by a PCET pathway.[14] The present experimental observations that surface-anchored phosphates can change the ORR to a four-electron reduction on TiO_2 lead to the hypothesis that the surface phosphates may provide acid/base sites and deliver protons for the reduction of O_2. To verify this hypothesis, instead of phosphates, the effect of other weak organic acids, such as L-glutamic acid (GA), malonic acid (MA), acetic acid (AA), and propionic acid (PA) was further examined. As shown in Figure 4, in the presence of all these acids, similar to the above phosphate system, the cathodic currents for the ORR increased significantly, relative to the pristine TiO_2. Interestingly, for the H_2O_2 generation efficiency, the results were rather distinctive. GA and MA displayed similar behaviors to phosphates: the generation of H_2O_2 was remarkably suppressed. In contrast, the influence of AA and PA on the H_2O_2 formation efficiency was quite minimal.

Phosphate or carboxylate groups are the most common linking groups to bind catalysts or chromophores onto metal oxide surfaces, and they were strongly adsorbed on the TiO_2 surface.[21–24] Note that phosphates, GA and MA are all polyprotic acids, while AA and PA are monocarboxylic acids. For polyprotic acids, although their adsorption modes on metal oxide are complex, it is possible for them to attach on the TiO_2 surface through one carboxylate, while the rest of carboxylate or the amide (in GA) groups are pendant on the surface. Such a structural motif is analogous to the catalytic center of the heme hydroperoxidase enzymes, such as cytochrome P450[10] and the so-called Hangman porphyrin,[12] where an acid–base functional group (amino acid residues or weak acid/base) is "hanged" over the face of the active center to deliver protons to the reaction center, thus achieving concerted $4e^-/4H^+$ reduction of O_2 to H_2O. Likewise, polyprotic acids could provide the pendant proton relays to bypass the single-electron reduction transformations through an oriented hydrogen-bonding network on the oxide surface

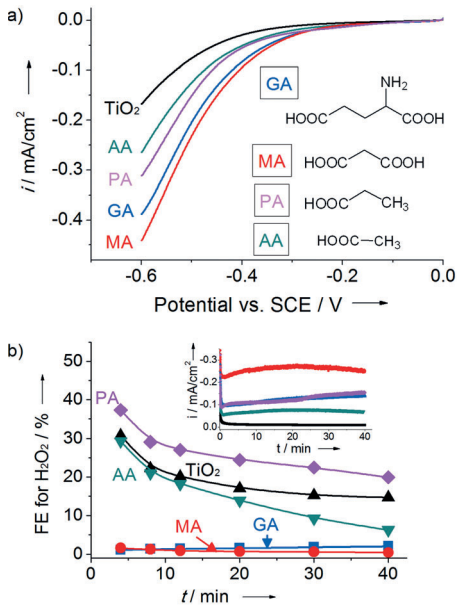

Figure 4. a) Linear sweep voltammetry of a TiO_2 film in O_2-saturated 0.1 M $NaClO_4$ solutions (pH 3.5) in the absence of and the presence of 4 mM organic acids. b) Faradaic efficiency (FE) for H_2O_2 during the steady-state electrolysis at −0.5 V (vs. SCE) and the current density (Inset) for TiO_2 film with or without 4 mM organic acids (L-glutamic acid (GA), malonic acid (MA), acetic acid (AA), propionic acid (PA)) in 0.1 M $NaClO_4$ electrolyte (pH 3.5).

(Scheme 1 a). In contrast, the surface-adsorbed monocarboxylic acids, such as AA and PA, lack the pendant acid/base group for such a reduction pathway, as the only available carboxylic group is used to anchor to the surface (Scheme 1 b). The absence of significant effects of these monocarboxylic acids on the formation efficiency of H_2O_2 highlights the important role of pendant proton relays in controlling the ORR pathway on TiO_2 surface. On the other hand, after anchoring of carboxylic acids, a higher local surface proton concentration relative to pristine TiO_2 surface is expected notwithstanding the pH values (3.5) being the same as that of the bulk solutions, as the adsorption of carboxylate acid on the TiO_2 surface is dissociative. The high surface proton concentration could probably be responsible for the enhanced reduction of O_2 with these acids (Figure 4). Different from the adsorbed polyprotic acids with pendant acid/base sites, however, all the steps in the ORR process [Eqs. (1)–(5)] should be accelerated equally by the unspecific distribution of proton around the reduction center. This situation may be a reasonable explanation for the observation that, in the presence of monocarboxylic acids such as AA and PA, the formation efficiency of H_2O_2 was not changed much in spite of the enhancement in the overall ORR rate.

The experimental finding that surface-pended proton relays can switch the ORR to four-electron reduction on TiO_2 is clearly of practical importance, as in terms of separation and recycling of catalysts the reaction on a surface is more desirable than in a homogeneous system. The role of surface-pendant proton relays demonstrated in this study could be applied to the design and development of efficient ORR heterogeneous catalysts. The effect of surface proton relays on ORR could also be expanded to other PECT reactions, such as catalytic CO_2 reduction, or the reduction of H_2O to hydrogen on the oxide surface. We also believe that a similar proton relay effect plays important roles in the high ORR reactivities of doped carbon materials,[25–27] where the dopants (for example, N) and residual carbonoxylic, hydroxy, and phenolic groups can provide plenty of pendant acid/base sites for the cleavage of O–O bonds.

Received: May 24, 2013
Published online: July 19, 2013

Keywords: oxygen reduction reaction · pendant proton relay · photocatalysis · titanium dioxide

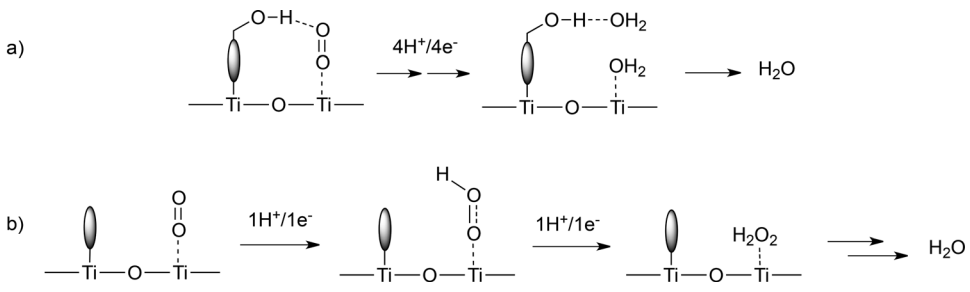

Scheme 1. The oxygen reduction on a TiO_2 surface: a) with adsorbed polyprotic acids as pendant proton relays, b) with adsorbed monoprotic acids in the absence of extra acid/base sites. Gray oval = adsorbed acid.

[1] A. Fujishima, X. T. Zhang, D. A. Tryk, *Surf. Sci. Rep.* **2008**, *63*, 515–582.
[2] X. Chen, S. S. Mao, *Chem. Rev.* **2007**, *107*, 2891–2959.
[3] C. C. Chen, W. H. Ma, J. C. Zhao, *Chem. Soc. Rev.* **2010**, *39*, 4206–4219.
[4] X. J. Lang, H. W. Ji, C. C. Chen, W. H. Ma, J. C. Zhao, *Angew. Chem.* **2011**, *123*, 4020–4023; *Angew. Chem. Int. Ed.* **2011**, *50*, 3934–3937.
[5] X. J. Li, W. S. Jenks, *J. Am. Chem. Soc.* **2000**, *122*, 11864–11870.
[6] Y. Li, B. Wen, C. L. Yu, C. C. Chen, H. W. Ji, W. H. Ma, J. C. Zhao, *Chem. Eur. J.* **2012**, *18*, 2030–2039.
[7] Y. V. Geletii, C. L. Hill, R. H. Atalla, I. A. Weinstock, *J. Am. Chem. Soc.* **2006**, *128*, 17033–17042.
[8] M. Teranishi, S. I. Naya, H. Tada, *J. Am. Chem. Soc.* **2010**, *132*, 7850–7851.
[9] R. Cai, Y. Kubota, A. Fujishima, *J. Catal.* **2003**, *219*, 214–218.
[10] J. Rosenthal, D. G. Nocera, *Acc. Chem. Res.* **2007**, *40*, 543–553.
[11] D. R. Weinberg, C. J. Gagliardi, J. F. Hull, C. F. Murphy, C. A. Kent, B. C. Westlake, A. Paul, D. H. Ess, D. G. McCafferty, T. J. Meyer, *Chem. Rev.* **2012**, *112*, 4016–4093.
[12] D. K. Dogutan, S. A. Stoian, R. McGuire, M. Schwalbe, T. S. Teets, D. G. Nocera, *J. Am. Chem. Soc.* **2011**, *133*, 131–140.
[13] C. T. Carver, B. D. Matson, J. M. Mayer, *J. Am. Chem. Soc.* **2012**, *134*, 5444–5447.

[14] J. N. Schrauben, R. Hayoun, C. N. Valdez, M. Braten, L. Fridley, J. M. Mayer, *Science* **2012**, *336*, 1298 – 1301.
[15] D. B. Thuan, A. Kimura, S. Ikeda, M. Matsumura, *J. Am. Chem. Soc.* **2010**, *132*, 8453 – 8458.
[16] L. Q. Jing, J. Zhou, J. R. Durrant, J. W. Tang, D. Liu, H. Fu, *Energy Environ. Sci.* **2012**, *5*, 6552 – 6558.
[17] D. Zhao, C. C. Chen, Y. F. Wang, H. W. Ji, W. H. Ma, L. Zang, J. C. Zhao, *J. Phys. Chem. C* **2008**, *112*, 5993 – 6001.
[18] H. Sheng, Q. Li, W. H. Ma, H. W. Ji, C. C. Chen, J. C. Zhao, *Appl. Catal. B* **2013**, *138 – 139*, 212 – 218.
[19] C. J. Fecenko, H. H. Thorp, T. J. Meyer, *J. Am. Chem. Soc.* **2007**, *129*, 15098 – 15099.
[20] Z. F. Chen, J. J. Concepcion, X. Q. Hu, W. T. Yang, P. G. Hoertz, T. J. Meyer, *Proc. Natl. Acad. Sci. USA* **2010**, *107*, 7225 – 7229.
[21] P. J. Hotchkiss, S. C. Jones, S. A. Paniagua, A. Sharma, B. Kippelen, N. R. Armstrong, S. R. Marder, *Acc. Chem. Res.* **2012**, *45*, 337 – 346.
[22] Z. Chen, J. J. Concepcion, J. W. Jurss, T. J. Meyer, *J. Am. Chem. Soc.* **2009**, *131*, 15580 – 15581.
[23] D. L. Ashford, W. J. Song, J. J. Concepcion, C. R. K. Glasson, M. K. Brennaman, M. R. Norris, Z. Fang, J. L. Templeton, T. J. Meyer, *J. Am. Chem. Soc.* **2012**, *134*, 19189 – 19198.
[24] B. O'Regan, M. Gratzel, *Nature* **1991**, *353*, 737 – 740.
[25] M. Jahan, Q. Bao, K. P. Loh, *J. Am. Chem. Soc.* **2012**, *134*, 6707 – 6713.
[26] K. Gong, F. Du, Z. Xia, M. Durstock, L. Dai, *Science* **2009**, *323*, 760 – 764.
[27] I. Y. Jeon, H. J. Choi, S. M. Jung, J. M. Seo, M. J. Kim, L. M. Dai, J. B. Baek, *J. Am. Chem. Soc.* **2013**, *135*, 1386 – 1393.

